

Simple El Niño prediction scheme using the signature of climate time series

Nozomi Sugiura ¹

Shinya Kouketsu ¹

¹Research and Development Center for Global Change, Japan Agency for Marine-Earth Science and Technology, Yokosuka, Japan

Key Points:

- A simple statistical El Niño prediction model was constructed.
- We applied machine learning based on a faithful representation of the past climate time series.
- The model has considerable skill and provides information about the sequence of climate events that tends to change the NINO3.4 sea surface temperatures.

Abstract

El Niño is a typical example of a coupled atmosphere-ocean phenomenon, but it is not yet clear whether it can be described quantitatively by a correlation between relevant climate events. We present an El Niño prediction model based on machine learning using the time series of climate indices. By transforming the multidimensional time series into the path signature, we were able to properly evaluate the order and nonlinearity of climate events, which allowed us to achieve good forecasting skill (mean square error = 0.596 for 6-month prediction). In addition, it is possible to provide information about the sequence of climate events that tend to change the future NINO3.4 sea surface temperatures. In our forecasting experiment, changes in the North Pacific Index and several NINO indices were found to be important precursors. The result suggests that El Niño is predictable in some extent just by the correlation of climate events.

1 Introduction

El Niño is an important climate phenomenon, with an immense socio-economic impact; its onset/offset mechanism has been drawing intense scientific interest for many years (e.g., Neelin et al., 1998; Wallace et al., 1998; Timmermann et al., 2018). The prediction of El Niño events is still under investigation from various perspectives, including statistical inference from past time series of climate records and results from climate models, initialization from climate models, and data assimilation using oceanic or coupled atmospheric-oceanic models.

Although previous studies suggest that the predictions with expensive climate models outperform purely statistical predictions (e.g. Wu et al., 2021), statistical prediction still seems to have value because of its simplicity (e.g., Penland & Magorian, 1993). Recently, elaborate and quite skillful predictions have been performed based on machine learning, or deep learning, with the use of past oceanic sea surface temperatures (SSTs) and subsurface information (Wang et al., 2020; Ham et al., 2019). Hu et al. (2021) carefully evaluated the climate network method that utilizes the relationship between spatio-temporal points to conclude that it has some prediction skill over one year. Dijkstra et al. (2019) reported that machine learning models can improve the prediction skill over an year. Nonetheless, few practical prediction studies have employed only the series of multi-dimensional climate indices as learning datasets. As a remarkable exception, Yan et al. (2020) used only the NINO3.4 index and the Southern Oscillation index to successfully perform a skillful prediction of the NINO3.4 index by using temporal convolutional network. Furthermore, a possible disadvantage of statistical predictions is that they typically provide little information about the correlations among these climate events through their evolution.

In this regard, we propose a new statistical method that is simple but considerably skillful, and provides process information to explain how climate events evolved. This study was conducted to develop a practical El Niño prediction scheme based on machine learning using past time series of climate indices. The key ingredient that enables the faithful interpretation of the past time series, including their nonlinearities, is the signature of paths, which is a central concept in rough path theory (Lyons et al., 2007).

Although there have been several papers on the methodology of time series analysis using the signature method (e.g., Morrill et al., 2021), there found no application of the method to global-scale climate events, and thus this paper opens a new field of research in geosciences.

2 Method

In this study, we apply a supervised learning to a time series of past climate indices, utilizing the fact that each segment of time series, as explanatory variables, is equipped with a future values at that time, as objective variables. The most striking aspect of the proposed method is to transform each segment of the time series into the signature. Therefore, our case study just employs the simplest setting utilizing the signature method to concentrate on the proof-of-the-concept. In this section, after explaining the theoretical basis why the signatures is relevant, we show the machine learning procedure based on that theory, and discuss how to interpret the results. Finally, we show the parameters used.

2.1 Approximating a function on a set of paths

In prediction study based on learning of time series, it is of crucial to properly construct a predictor that link past time series segments to future values. A predictor is represented as a continuous function on a set of multidimensional paths. In order to secure the performance of the predictor, it is essential to choose an appropriate basis for the function of the path because it determines the expressive power of the function. Note that our concern is not the basis for a path but for a function of paths. In this sense, the most mathematically justified candidate for the basis is the signature (Lyons et al., 2007).

For a d -dimensional path $X = X_{[s,t]} : [s, t] \rightarrow \mathbb{R}^d$ that maps τ to X_τ , the n -th iterated integrals are defined recursively as (Lyons et al., 2007):

$$\mathcal{S}^{(0)}(X_{[s,t]}) = 1, \quad (1)$$

$$\mathcal{S}^{(i_1 \cdots i_n)}(X_{[s,t]}) = \int_s^t \mathcal{S}^{(i_1 \cdots i_{n-1})}(X_{[s,t_n]}) dX_{t_n}^{(i_n)}, \quad i_1, \cdots, i_n = 1, \cdots, d. \quad (2)$$

The signature $\mathcal{S}(X)$ of path X is the collection of all the iterated integrals, and the operation $\mathcal{S} : X \mapsto \mathcal{S}(X)$ is called the signature transform. In particular, its truncation up to the n -th iterated integrals is called a step- n signature, $\mathcal{S}_n(X)$.

Now, let $C(K, \mathbb{R})$ be the space of a continuous function on a compact set K of paths. $A \subset C(K, \mathbb{R})$ is defined as

$$A = \left\{ g : K \ni X \mapsto g(X) = \sum_I w^{(I)} \mathcal{S}^{(I)}(X) \in \mathbb{R} \mid w^{(I)} \in \mathbb{R}, I : \text{multi-indices} \right\}, \quad (3)$$

where, the multi-indices run across $I = (), (i_{1,1}), \cdots, (i_{n,1} \cdots i_{n,n})$; $i_{j,k} = 1, \cdots, d$ for arbitrary $n > 0$. Then, A satisfies the following conditions:

1. Because step- n signature transform $K \ni X \mapsto \mathcal{S}_n(X)$ is continuous for any $n > 0$, $A \subset C(K, \mathbb{R})$.
2. $g_1, g_2 \in A$ and $\lambda_1, \lambda_2 \in \mathbb{R} \implies \lambda_1 g_1 + \lambda_2 g_2 \in A$.
3. Constant-valued function $\mathbf{1} \in A$.
4. Based on the shuffle identities (Lyons et al., 2007), $g_1, g_2 \in A \implies g_1 g_2 \in A$.
5. Based on the uniqueness theorem (Levin et al., 2013), for all $X, Y \in A$ with $X \neq Y$, there exists $g \in A$ that satisfies $g(X) \neq g(Y)$.

From these conditions, we can apply the Stone-Weierstrass theorem (Stone, 1937) to the subset A and conclude that A is dense in $C(K, \mathbb{R})$, which means that any function $f \in C(K, \mathbb{R})$ is uniformly approximated by a function $g \in A$ with arbitrary accuracy (Levin et al., 2013).

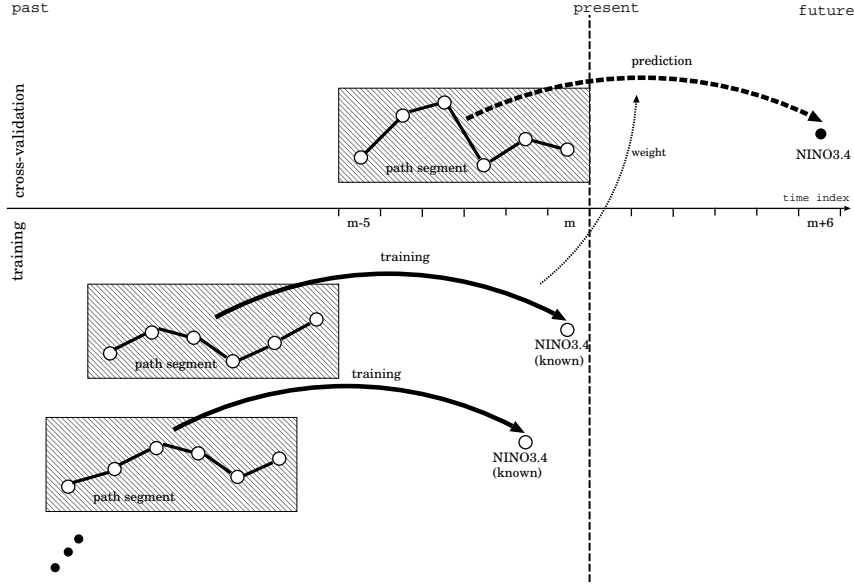


Figure 1. Schematic view of training and prediction flow, assuming that $m_b=m_a=6$. Hatched squares represent transforming into the signature. Predicted value at time index $m+6$ will be compared with the validation data if available.

From the above reasoning, we construct the predictor as a linear combination of iterated integrals for each segment of the multi-dimensional time series. We computed the signature by using Python library `esig` (Kormilitzin, 2017).

2.2 Procedure for machine learning of time-series

In the proposed approach, the predictor is constructed as follows. Suppose we have a time series of several climate indices defined at each calendar month of t_m , $m = 1, 2, \dots, M$. Any segment of the time series over a period of time, say six months, can be viewed as a multidimensional path, which can be represented by the signature.

For this supervised learning, the object variable is the NINO3.4 index y_{m+m_a} at time $\tau = t_{m+m_a}$, while the explanatory variables x_m are the iterated integrals for the segment of time series X in the period $[t_{m-m_b+1}, t_m]$. The approximation property described in the previous section allows us to express the object variable as a linear combination of the explanatory variables:

$$y_{m+m_a} = y_m + \langle w_m, x_m \rangle + \epsilon, \quad (4)$$

$$x_m := \mathcal{S}_n(X_{[t_{m-m_b+1}, t_m]}), \quad (5)$$

where $\mathcal{S}_n(X_{[t_0, t_1]})$ denotes the order- n signature for the d -dimensional time series in the interval $[t_0, t_1]$, $\langle a, b \rangle$ denotes the scalar product $\sum_I a^{(I)} b^{(I)}$, $w_m = \{w_m^{(I)} | I = \text{multi-indices}\}$ is the weight vector for the predictor, ϵ is a random variable representing prediction error, t_m is the starting time of the prediction, t_{m-m_b+1} is the starting point of the path segment, and t_{m+m_a} is the target time for prediction. Before converting into the signature, a zero vector is added at the beginning of each series $X_{[t_{m-m_b+1}, t_m]}$ to account for the magnitude of the value at the starting point (Morrill et al., 2021).

In the control case, we instead used the time series as it is without converting it into the signature:

$$x_m := X_{[t_{m-m_b+1}, t_m]} = (X_{t_{m-m_b+1}}, X_{t_{m-m_b+2}}, \dots, X_{t_m}). \quad (6)$$

This corresponds to an auto-regressive (AR) model.

Using the training dataset available up to time t_m :

$$D_m = \{(x_\mu, y_{\mu+m_a} - y_\mu) \mid \mu \in [m_b, m - m_a]\}, \quad (7)$$

we first estimate the optimal weight $w = w_m$ that minimizes the cost function with an L_1 -penalty term:

$$J_m(w) = \frac{1}{2|D_m|} \sum_{\mu=m_b}^{m-m_a} (y_{\mu+m_a} - y_\mu - \langle w, x_\mu \rangle)^2 + \alpha \sum_I |w^{(I)}|, \quad (8)$$

where $|D_m| = m - m_a - m_b + 1$ is the number of samples in D_m , and I is the multi-index. The optimization problem is solved by the Lasso model fit with least angle regression (Pedregosa et al., 2011), which is suitable for problems with many parameters. We then predict a future NINO3.4 index y_{m+m_a} as $\hat{y}_{m+m_a} = y_m + \langle w_m, x_m \rangle$. We repeat the above procedure by moving the starting time of prediction t_m .

Figure 1 shows the schematic view of training and prediction flow. In this flow, the weight w_m is obtained by using the training data set D_m , and then the prediction from time t_m using the signature x_m yields the value \hat{y}_{m+m_a} , which is subject to comparison with the validation data y_{m+m_a} . Note that the size of the training data $|D_m| = m - m_a - m_b + 1$ depends on the starting time t_m . The prediction error can be obtained from the statistics of $\hat{y}_{m+m_a} - y_{m+m_a}$ for various starting time. By taking this approach, where trainings and forecasts are done progressively by moving the starting time of the forecast hiding future at that moment, each forecast is assured to be a fair cross-validation.

2.3 Diagnosing the dominant event sequences

One difficulty with regular machine learning is that it does not provide sufficient reasoning for the results. However, the signature-based method allows us to mathematically extract from the path, the properties that are important in the prediction.

To diagnose the dominant event sequences that contribute to the prediction, we compute the standard partial regression coefficients (SPRCs) $r_m^{(I)}$, which represent the sensitivity of normalized value $y_{\mu+m_a}$ in the future to each component of the normalized signature $x_\mu^{(I)}$ in the past, as

$$r_m^{(I)} = \frac{\sigma_{x_m^{(I)}}}{\sigma_{y_m}} w_m^{(I)}, \quad (9)$$

where σ_{y_m} and $\sigma_{x_m^{(I)}}$ denote the standard deviations of $y_{\mu+m_a} - y_\mu$ and $x_\mu^{(I)}$, respectively, among the samples in D_m , which represents the learning data in the period from time t_1 to time t_m .

2.4 Setting of experimental parameters

We use a climate time series comprised of $d = 12$ indices in Table 1 retrieved from *Climate Timeseries at PSL* (2021). The time series starts at t_1 (January of 1900), and ends at t_{1459} (July of 2021).

The standard lead time for prediction is 6-month ($m_a = 6$), whereas each past segment is of length 6-month ($m_b = 6$). The experiment duration is from the prediction starting at t_{961} (January of 1980), to the one starting at t_{1453} (January of 2021).

Table 1. Twelve climate indices and their abbreviations

Abbrev.	Climate Indices
NINO34	Nino 3.4 (5N-5S, 170W-120W) SST (Rayner et al., 2003)
NINO12	Nino 1+2 (0-10S, 90W-80W) SST (Rayner et al., 2003)
NINO3	Nino 3 (5N-5S, 150W-90W) SST (Rayner et al., 2003)
NINO4	Nino 4 (5N-5S, 160E-150W) SST (Rayner et al., 2003)
DMI	Dipole Mode Index (Hameed & Yamagata, 2003)
AMO	Atlantic Multidecadal Oscillation index (Enfield et al., 2001)
NPI	North Pacific Index (Trenberth & Hurrell, 1994)
SOI	Southern Oscillation Index (Ropelewski & Jones, 1987)
NAO	North Atlantic Oscillation (NAO) index (Jones et al., 1997)
TPI	Tripole Index (Henley et al., 2015)
AO	Arctic Oscillation index (Thompson & Wallace, 1998)
MON	Date elapsed (mid-day in month divided by 365)

We use iterated integrals up to level $n = 3$, which means that the total number of terms in the linear combination is $N = (d^{n+1} - 1)/(d - 1) = 1885$, and the intensity of the L_1 penalty term has been tuned to $\alpha = 2.0$.

3 Results

Figure 2 shows the result of 6-month prediction. The prediction error for each target month is shown in Fig. 3. It is obvious that the predictions for July to September were much better than those in the control case; however, they were comparable in the other months. The overall prediction skill was 0.596K for the signature case and 0.663K for the control case. For comparison with the operator-theoretic technique Wang et al. (2020) and linear inverse model (LIM), the root-mean square (rms) errors for 6-month prediction in the period from 1998 to 2017 were computed. The signature model, AR model, KAF (kernel analog forecasting) model, and LIM had rms values of 0.617, 0.686, 0.62, and 0.75K, respectively. This comparison suggests that the signature model has a skill comparable to that of the KAF model.

The spring prediction barrier is defined in Lai et al. (2018) as follows: “... models have problems in predicting Boreal winter tropical Pacific sea surface temperature (SST) when forecasts start in Boreal spring (February–May). This is called the spring predictability barrier.” Similarly, Zheng and Zhu (2010) pointed out that “... errors have the largest values and the fastest growth rates initialized before and during the NH spring.” In light of these definitions, the spring predictability barrier, i.e., poor prediction skill when starting from February and March, seems to disappear as indicated by the rms error values in the target months of August to September.

Table 2 shows the dominant event sequences among iterated integrals. The events with the first to the third index are shown in each row. If the same index appears twice in a row, then the event is intense. The top sequence in the period from 1900 to 2020 is an intense NPI change followed by a Niño 1+2 SST change. The key indices are NPI and various NINO indices. In particular, NPI, an atmospheric process, is involved in all the dominant sequences, which should be a manifestation that El Niño is a coupled atmospheric-oceanic process. Summarizing the above, fig. 4 illustrates how the dominant climate events occur that will lead to changes in the future NINO3.4.

Table 2. Top five dominant event sequences among iterated integrals. “1st” means the first index for the corresponding degree-3 iterated integral: $x^{(i_1 i_2 i_3)} = \int_0^1 \int_0^{t_3} \int_0^{t_2} dX_{t_1}^{(i_1)} dX_{t_2}^{(i_2)} dX_{t_3}^{(i_3)}$. Events happen from first to third. If the same index appears twice in a row, then the event is intense. “SPRC” represents the standard partial regression coefficients (Eq. 9).

No.	Learning data from Jan. 1900 to Dec. 1999				Learning data from Jan. 1900 to Dec. 2020			
	SPRC $r_t^{(i_1 i_2 i_3)}$	Indices in iterated integrals			SPRC $r_t^{(i_1 i_2 i_3)}$	Indices in iterated integrals		
		1st (i_1)	2nd (i_2)	3rd (i_3)		1st (i_1)	2nd (i_2)	3rd (i_3)
1	5.55	NPI	NINO3	NPI	4.53	NPI	NPI	NINO12
2	-3.70	NINO3	NPI	NPI	-4.17	NINO34	NINO34	NPI
3	3.63	NPI	NPI	NINO12	-3.37	NPI	NINO34	NINO12
4	-3.57	NINO34	NINO34	NPI	-3.25	NINO34	NPI	NINO12
5	3.34	NINO34	NPI	NPI	2.88	NPI	NINO3	NPI

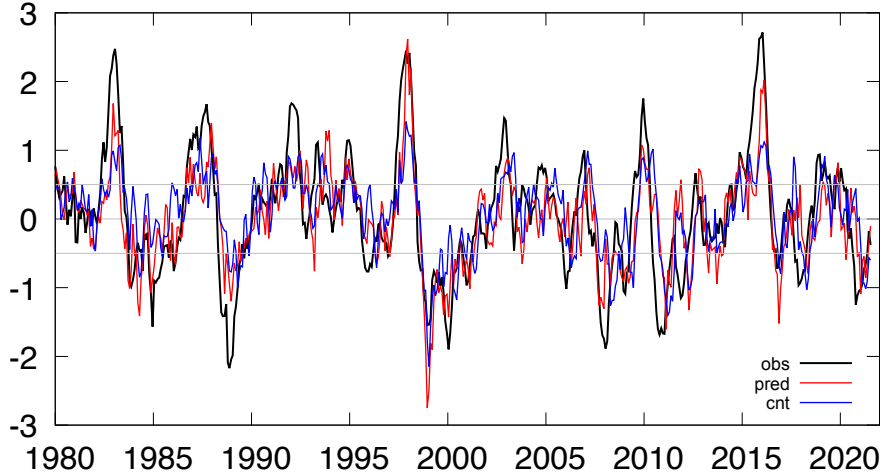


Figure 2. Comparison of NINO3.4 for 6-month predictions. Red: signature case; blue: control case. Horizontal axis is the target month, and vertical axis is the deviation from verification data.

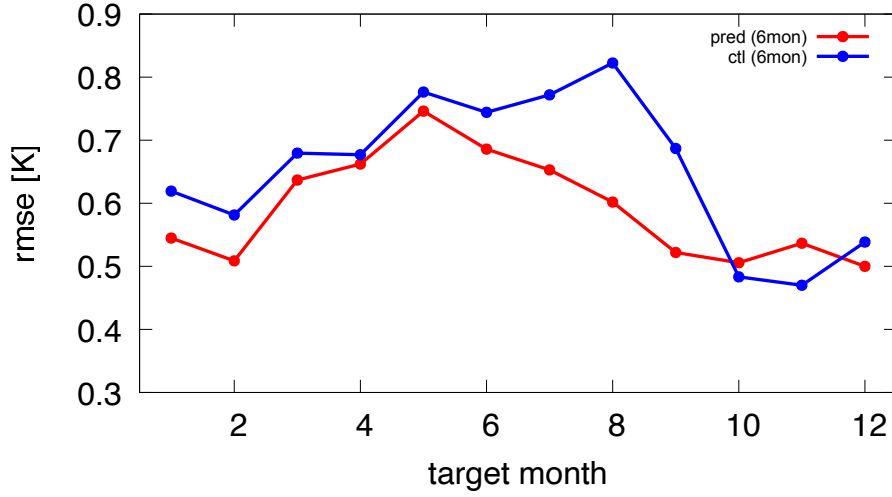


Figure 3. Prediction error for each target month. Red: signature case, blue: control case. Horizontal axis is the target month (1 = January, 2 = February, ..., 12=December), and vertical axis is rms error in K.

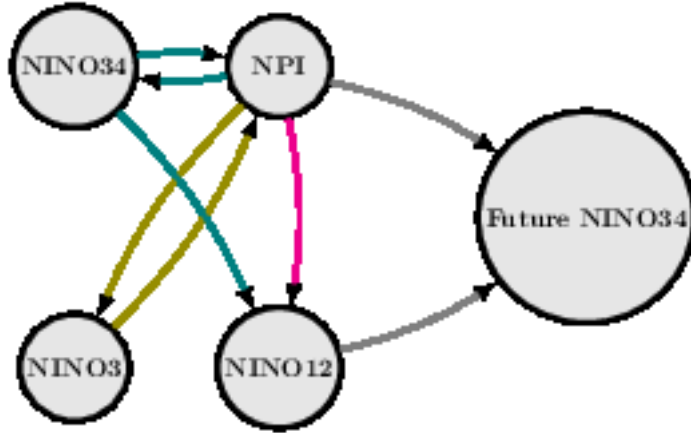


Figure 4. Typical climate event flows for predicting future Nino3.4 index. Arrows indicate time order. Key indices include NINO12 (Nino1+2 SST), NINO34 (Nino3.4 SST), NINO4 (Nino4 SST), and NPI (North Pacific Index).

4 Conclusions

We developed a model that can statistically predict El Niño using only the time series of past multidimensional climate indices. By converting the time series into the signature, the accuracy of the machine learning algorithm can be improved, and thereby the NINO3.4 SST can be predicted to some extent six months in advance. An important byproduct of this approach is that the correlation of climate events can be read from the dominant iterative integral. For example, it was suggested that variations in the NPI, NINO12, and other indices occur in a certain order, which leads to variations in the NINO3.4 SST. It was also found that the signature method can learn the nonlinear development of El Niño more accurately than the traditional AR model, and thus, is less sensitive to the spring barrier of predictability. Future research is required to improve the scheme by incorporating more detailed oceanographic information, evaluating uncertainties, and considering other factors.

The predictions obtained by this method are not marked with error bars, but since we know the prediction error for each month as shown in Fig. 3, we can consider these values as the prediction error. However, since it is not possible to give a forecast error for each forecast individually, an ensemble could be created by bootstrapping or other methods to improve this point, which may also lead to a factory for forecast accuracy.

The length of the path segment used for the 6-month forecast, 6 months, was confirmed in preliminary experiments (not shown) to be appropriate, but the length of the path segment required for forecasts with other lead times may be different. It is also necessary to confirm whether the 3-stage signature is optimal.

Dominant iterated integral for prediction may change from time to time depending on the period covered as shown in Table 2. It needs to be carefully considered how this relates to the decadal changes in the Niño mechanism. These points remain as future work.

Acknowledgments

This study was funded by JST-PROJECT-20218919. The code used for the machine learning will be available soon on github.

References

- Climate Timeseries at PSL*. (2021). Retrieved from https://psl.noaa.gov/gcos_wgsp/Timeseries/
- Dijkstra, H. A., Petersik, P., Hernández-García, E., & López, C. (2019). The application of machine learning techniques to improve El Niño prediction skill. *Frontiers in Physics*, 7, 153.
- Enfield, D. B., Mestas-Núñez, A. M., & Trimble, P. J. (2001). The atlantic multi-decadal oscillation and its relation to rainfall and river flows in the continental u.s. *Geophysical Research Letters*, 28(10), 2077-2080. Retrieved from <https://agupubs.onlinelibrary.wiley.com/doi/abs/10.1029/2000GL012745> doi: <https://doi.org/10.1029/2000GL012745>
- Ham, Y.-G., Kim, J.-H., & Luo, J.-J. (2019). Deep learning for multi-year enso forecasts. *Nature*, 573(7775), 568–572. doi: <https://doi.org/10.1038/s41586-019-1559-7>
- Hameed, S., & Yamagata, T. (2003, 12). Possible impacts of indian ocean dipole mode events on global climate. *Climate Research - CLIMATE RES*, 25, 151-169. doi: 10.3354/cr025151
- Henley, B. J., Gergis, J., Karoly, D. J., Power, S., Kennedy, J., & Folland, C. K. (2015, December). A Tripole Index for the Interdecadal Pacific Oscillation. *Climate Dynamics*, 45(11-12), 3077-3090. doi: 10.1007/s00382-015-2525-1

- Hu, X., Eichner, J., Faust, E., & Kantz, H. (2021). Benchmarking prediction skill in binary el niño forecasts. *Climate Dynamics*, 1–15.
- Jones, P. D., Jonsson, T., & Wheeler, D. (1997). Extension to the north atlantic oscillation using early instrumental pressure observations from gibraltar and south-west iceland. *International Journal of Climatology*, 17(13), 1433–1450. doi: [https://doi.org/10.1002/\(SICI\)1097-0088\(19971115\)17:13<1433::AID-JOC203>3.0.CO;2-P](https://doi.org/10.1002/(SICI)1097-0088(19971115)17:13<1433::AID-JOC203>3.0.CO;2-P)
- Kormilitzin, A. (2017). *the-signature-method-in-machine-learning*. <https://github.com/kormilitzin/>.
- Lai, A. W.-C., Herzog, M., & Graf, H.-F. (2018). Enso forecasts near the spring predictability barrier and possible reasons for the recently reduced predictability. *Journal of Climate*, 31(2), 815–838.
- Levin, D., Lyons, T., & Ni, H. (2013, September). Learning from the past, predicting the statistics for the future, learning an evolving system. *ArXiv e-prints*.
- Lyons, T. J., Caruana, M., & Lévy, T. (2007). *Differential Equations Driven by Rough Paths* (Vol. 1908). Springer.
- Morrill, J., Fermanian, A., Kidger, P., & Lyons, T. (2021). *A Generalised Signature Method for Multivariate Time Series Feature Extraction*.
- Neelin, J. D., Battisti, D. S., Hirst, A. C., Jin, F.-F., Wakata, Y., Yamagata, T., & Zebiak, S. E. (1998). Enso theory. *J. Geophys. Res.*, 103, 14 261–14 290.
- Pedregosa, F., Varoquaux, G., Gramfort, A., Michel, V., Thirion, B., Grisel, O., ... Duchesnay, E. (2011). Scikit-learn: Machine learning in Python. *Journal of Machine Learning Research*, 12, 2825–2830.
- Penland, C., & Magorian, T. (1993). Prediction of Niño 3 Sea Surface Temperatures Using Linear Inverse Modeling. *Journal of Climate*, 6(6), 1067 - 1076. Retrieved from https://journals.ametsoc.org/view/journals/clim/6/6/1520-0442_1993_006_1067_ponsst_2_0_co_2.xml doi: 10.1175/1520-0442(1993)006<1067:PONSST>2.0.CO;2
- Rayner, N. A., Parker, D. E., Horton, E. B., Folland, C. K., Alexander, L. V., Rowell, D. P., ... Kaplan, A. (2003). Global analyses of sea surface temperature, sea ice, and night marine air temperature since the late nineteenth century. *Journal of Geophysical Research: Atmospheres*, 108(D14). Retrieved from <https://agupubs.onlinelibrary.wiley.com/doi/abs/10.1029/2002JD002670> doi: <https://doi.org/10.1029/2002JD002670>
- Ropelewski, C. F., & Jones, P. D. (1987). An extension of the tahiti–darwin southern oscillation index. *Monthly weather review*, 115(9), 2161–2165.
- Stone, M. (1937). Applications of the theory of boolean rings to general topology. *Transactions of the American Mathematical Society*, 41, 375–481.
- Thompson, D. W. J., & Wallace, J. M. (1998). The arctic oscillation signature in the wintertime geopotential height and temperature fields. *Geophysical Research Letters*, 25(9), 1297–1300. Retrieved from <https://agupubs.onlinelibrary.wiley.com/doi/abs/10.1029/98GL00950> doi: <https://doi.org/10.1029/98GL00950>
- Timmermann, A., An, S.-I., Kug, J.-S., Jin, F.-F., Cai, W., Capotondi, A., ... others (2018). El niño–southern oscillation complexity. *Nature*, 559(7715), 535–545.
- Trenberth, K., & Hurrell, J. (1994). Decadal atmosphere-ocean variations in the Pacific. *Climate Dynamics*, 9, 303–319. doi: <https://doi.org/10.1007/BF00204745>
- Wallace, J. M., Rasmusson, E. M., Mitchell, T. P., Kousky, V. E., Sarachik, E. S., & von Storch, H. (1998). On the structure and evolution of enso related climate variability in the tropical pacific: Lessons from toga. *J. Geophys. Res.*, 103, 14 241–14 259.
- Wang, X., Slawinska, J., & Giannakis, D. (2020). Extended-range statistical ENSO prediction through operator-theoretic techniques for nonlinear dynamics. *Sci*

- Rep.*, 10(1), 2636. doi: 10.1038/s41598-020-59128-7
- Wu, X., Okumura, Y. M., Deser, C., & DiNezio, P. N. (2021). Two-Year Dynamical Predictions of ENSO Event Duration during 1954–2015. *Journal of Climate*, 34(10), 4069 - 4087. Retrieved from <https://journals.ametsoc.org/view/journals/clim/34/10/JCLI-D-20-0619.1.xml> doi: 10.1175/JCLI-D-20-0619.1
- Yan, J., Mu, L., Wang, L., Ranjan, R., & Zomaya, A. Y. (2020). Temporal convolutional networks for the advance prediction of ENSO. *Scientific reports*, 10(1), 1–15.
- Zheng, F., & Zhu, J. (2010). Spring predictability barrier of ENSO events from the perspective of an ensemble prediction system. *Global and Planetary Change*, 72(3), 108–117.